TRANSITION TO OSCILLATORY MARANGONI CONVECTION IN LIQUID BRIDGES OF INTERMEDIATE PRANDTL NUMBER

M. Kawaji[1], S. Simic[1], G. Psofogiannakis[1], and S. Yoda[2]

[1]Dept. of Chemical Engineering and Applied Chemistry, University of Toronto, Toronto, Ontario M5S 3E5, Canada
[2]National Space Development Agency of Japan, 2-1-1 Sengen, Tsukuba, 305-8505, Japan

Marangoni convection experiments have been conducted with acetone (Pr = 4.3) and methanol (Pr = 6.8) liquid bridges to investigate the flow structures and temperature fields during transition from steady to oscillatory convection in a half floating zone. In particular, the effects of liquid evaporation on the onset of oscillatory flow were investigated by performing the experiments under different evaporation rates. The effects of horizontal vibrations with small amplitudes were also investigated to understand the magnitude of free surface oscillation induced by such vibrations. In all of the experiments, a test section with 7.0 mm diameter disks was constructed to enable reduction of the evaporation rate by a factor of 4 to 5 by providing a tight seal between the inside and outside of a quartz tube fitted around the liquid bridge. The liquid bridge height was changed from 2.0 mm to 4.5 mm, covering aspect ratios from 0.55 up to 1.3.

For acetone under reduced evaporation rates, the transition from steady to oscillatory convection was found to occur at disk temperature differences of 0.5 ~ 1.1 K, much less than 1.6 ~ 2.3 K for the partially open system. This difference in the critical temperature difference and corresponding critical Marangoni number data clearly showed the stabilizing effect of surface evaporation. The surface temperature profile for the partially open system also showed temperature inversion above the lower disk, where a cold region with a temperature below the cold disk temperature existed, as predicted by the linear stability analysis. On the other hand, the evaporation effect was found to be quite small for methanol, and the critical Marangoni numbers obtained agreed with the previous data for $NaNO_3$ with a similar Prandtl number. For both acetone and methanol, the critical Marangoni numbers obtained for an aspect ratio of unity agreed with the predictions of a linear stability analysis, which also correctly predicted the stabilization effect of surface evaporation and an increase in the critical Marangoni number.

The effects of forced vibration on the stability of a liquid bridge surface was also investigated by subjecting the acetone liquid bridge of 7.0 mm diameter to horizontal vibrations under an isothermal condition. The acceleration level was kept at 5 mG but the vibration frequency and amplitude were varied in the experiments. The response of the liquid bridge surface was recorded by a video camera and the surface motion was analyzed for different volume and aspect ratios. The results indicated existence of resonance frequencies at which the surface oscillates with large amplitudes, and a strong effect of the volume ratio on the oscillation amplitude. The maximum surface oscillation amplitude as high as 250 m was recorded at applied vibration frequencies of 4 and 12 Hz. The resonance frequencies at which the liquid bridge vibrated with large amplitudes decreased linearly with the height of the liquid bridge.

1. INTRODUCTION

Thermocapillary or Marangoni convection in a cylindrical liquid bridge formed between heated and cooled circular disks is important for understanding the transport processes involved in the floating zone crystal growth. In particular, the quality of crystals grown may be adversely affected when Marangoni convection undergoes transition from a steady to oscillatory state and the resulting temperature and velocity field fluctuations in the melt could cause striations to appear in the crystal.

Previously, many experiments on Marangoni convection in liquid bridges have been conducted mostly employing high Pr number fluids. These results have indicated that the critical Marangoni number, at which steady to oscillatory flow transition occurs, varies with the Prandtl number, disk diameter, volume ratio and aspect ratio (Γ = height / radius) of the liquid bridge. On the other hand, numerical analyses of such experiments encounter considerable difficulties due to the reduction in the thermal boundary layer thickness at high Prandtl numbers and its implications for finer grid resolution.

The numerical difficulty associated with thin boundary layers is alleviated when Marangoni convection at intermediate Prandtl numbers up to about 7, is examined. Several experiments have been conducted in the past yielding data useful for verification of numerical results. Preisser et al. (1983) and Velten et al. (1991) have experimentally studied certain aspects of transition to oscillatory Marangoni convection for high temperature melts, KCl (Pr = 1) and $NaNO_3$ (Pr = 7). They measured the critical temperature difference, ΔT_c, and the frequency of temperature oscillations for a disk diameter of 6 mm and various aspect ratios. Chun and Wuest (1978) and Vargas (1982) have also reported critical Marangoni number data and other results for methanol (Pr = 7). Some of these experimental data have been used by Wanschura et al. (1995) and Leypolds et al. (2000) to compare with numerical linear stability analysis and direct numerical simulation results, respectively.

Regarding the oscillation mechanism, Kamotani et al. (1984) suggested that triple coupling among the velocity, temperature and surface deformation is responsible for high Pr fluids. Strong and weak convection periods would occur alternately at different radial planes and interact in such a way that the entire flow structure becomes non-axisymmetric. To what range of Prandtl numbers this postulated mechanism applies needs to be verified experimentally or by sufficiently precise numerical simulation.

More detailed data are needed on flow and thermal structures at the onset of oscillatory convection in liquid bridges of intermediate Prandtl number in order to gain further insights into the oscillatory Marangoni convection phenomena and to provide useful data for comparisons with numerical analyses. In particular, a significant influence of heat and mass transfer at the free surface has been pointed out by Velten et al. (1991), but no effort has been made to date to further quantify and analyze these effects.

To this end, Marangoni convection experiments have been conducted in the preceding year using acetone (Pr = 4.3), which is a volatile liquid and significant mass and heat transfer occurs at the liquid surface due to evaporation. Thus, it became necessary to study the effect of surface evaporation on transition from steady to oscillatory Marangoni convection by varying the evaporation rate. This year, a new test section was constructed so that different evaporation rates could be realized by placing a partially or tightly sealed enclosure around the liquid bridge with a diameter of 7.0 mm. Experiments were conducted under both reduced and strong evaporation rates using the photochromic dye activation and PIV methods of flow visualization and an infrared imager to monitor the liquid bridge surface temperature distribution. The same test section was also used for another medium Prandtl number fluid, methanol (Pr = 7), for one

aspect ratio. The data were analyzed to determine the effects of surface evaporation both on the flow structure and the critical Marangoni number.

An additional series of experiments was conducted this year to investigate the effect of horizontal vibrations on the stability of a liquid bridge surface. An acetone bridge with D = 7.0 mm was subjected to horizontal vibrations under an isothermal condition. The response of the liquid bridge surface to vibrations of varying frequency and amplitude was recorded by a video camera and the surface motion was analyzed for different volume and aspect ratios.

2. HORIZONTAL VIBRATION MODEL

In 2001, Ichikawa et al. proposed a model by which the resonance frequencies of liquid bridges of perfect cylindrical shape could be estimated. The model was based on a mass-spring-damper system and the following assumptions were made for the derivation of the equations:

- Liquid is Newtonian and the flow induced within the liquid bridge is laminar.
- The liquid bridge moves only in the horizontal direction. The shape of the horizontal cross-section remains circular at any height of the liquid bridge.
- Gravity effects are not considered.

According to the authors, the governing equation of motion for the liquid bridge surface is:

$$m\frac{d^2x}{dt^2} + 2mk\frac{dx}{dt} + m\omega_0{}^2 x = \frac{F_0}{m}\sin\omega t \qquad (1)$$

In equation 1 the symbols represent:

m: the moving mass of the liquid bridge.

k: a damping parameter caused by viscosity in the liquid bridge.

ω_0: a restoring force parameter (tends to bring deformed surface back to equilibrium shape).

x: the displacement of the free surface from the equilibrium position.

F_0: the magnitude of applied external force.

The analytical solution to equation 1 is given by:

$$x = Ae^{-kt}\cos(\sqrt{\omega_0{}^2 - k^2}\cdot t + \alpha) + \frac{1}{\sqrt{(\omega_0{}^2 - \omega^2)^2 + 4k^2\omega^2}}\frac{F_0}{m}\sin(\omega t - \delta) \qquad (2)$$

According to this equation, the amplitude of vibration of the liquid bridge surface is:

$$x_{amp.} = \frac{1}{\sqrt{(\omega_0{}^2 - \omega^2)^2 + 4k^2\omega^2}}\frac{F_0}{m} \qquad (3)$$

This term has a local maximum at:

$$\omega_{\mathrm{Res.}} = \sqrt{\omega_0{}^2 - 2k^2} \qquad (4)$$

The parameters m, k and ω_0 were subsequently estimated as follows.

Estimation of m (moving mass)

Ichikawa et al. (2001) considered a perfectly cylindrical shape and some volume fraction, B, to move due to horizontal vibration. The moving mass is then given by,

$$m = \frac{\rho\pi D^2 HB}{4} \qquad (5)$$

The authors noted that the parameter, B, could take a value between 0.5 and 1.0, depending on the type of motion involved. The rest of the parameters are:

ρ: density of the liquid,

D: diameter of the liquid bridge,

H: height of the liquid bridge.

Estimation of k (a damping parameter)

The shear stress in the liquid bridge, induced by the horizontal liquid motion is considered to be given by a linear velocity profile from zero at the upper and lower disks and a maximum value, *dx/dt*, at the mid-height:

$$\tau = \mu \frac{\partial u}{\partial z} = 2\mu \frac{dx/dt}{H}$$

where

τ: the shear stress,

μ: the liquid viscosity (6)

Ichikawa et al. (2001) compared equation 6 with the second term of equation 1:

$$2mk = \frac{2\mu}{H}\pi\left(\frac{D}{2}\right)^2 = \frac{\pi D^2}{2H}\mu \quad (7)$$

(8)

By substituting equation 5 for m:

$$k = \frac{\nu}{H^2}\frac{1}{B}$$

where:

ν: kinematic viscosity of the liquid $(= \frac{\mu}{\rho})$

Estimation of ω_0 (restoring force parameter)

The following assumptions were made in the derivation of the equations:

- The principal radii of the surface curvature at any height are the same as those at the mid-height of the liquid bridge.
- The amplitude of surface motion is negligible compared to the height of the liquid bridge.

After formulating the problem geometrically and applying Young-Laplace's equation to the system, Ichikawa et al. (2001) came up with the following equation:

$$m\omega_0^2 = \sigma D \frac{4}{H}\pi$$

From equation 9:

$$\omega_0 = \frac{4}{H}\sqrt{\frac{\sigma}{D\rho}\frac{1}{B}} \quad (10)$$

where

σ: surface tension of the liquid.

Substituting for m (eq.5), k (eq.8) and ω_0 (eq.10) in equation 4, the resonance fr (Eq.9) f a liquid bridge is given by:

$$\omega_{\text{Res.}} = \frac{1}{H}\sqrt{\frac{2}{B}\left(\frac{8\sigma}{D\rho} - \frac{\nu^2}{H^2 B}\right)} \tag{11}$$

where all the parameters have been previously defined.

The resonance frequency is then given by:

$$f_{\text{Res.}} = \frac{\omega_{\text{Res.}}}{2\pi} = \frac{1}{2\pi H}\sqrt{\frac{2}{B}\left(\frac{8\sigma}{D\rho} - \frac{\nu^2}{H^2 B}\right)} \tag{12}$$

It was observed that taking the actual physical properties of acetone, the last term of equation 12 can be neglected:

$$\frac{\nu^2}{H^2 B} \ll \frac{8\sigma}{D\rho}$$

Therefore, with B=1, equation 12 reduces to:

$$f_{\text{Res.}} = \frac{2}{\pi H}\sqrt{\frac{\sigma}{D\rho}} \tag{13}$$

The last assumption holds for any common liquids that can be practically encountered.

Also, substituting for the parameters in equation 3 (with B=1), one can obtain the surface oscillation amplitude as a function of the applied vibration frequency.

$$x_{amp.} = \frac{a_0}{\sqrt{\left[\frac{16}{H^2}\frac{\sigma}{D\rho} - (2\pi f)^2\right]^2 + 4\frac{\nu^2}{H^4}(2\pi f)^2}} \tag{14}$$

Ichikawa et al. (2001) investigated experimentally the validity of the proposed model using water as the test liquid. They found that the model under-predicted the experimental resonance frequency by 33% and attributed the difference to an experimental error (the existence of a bubble within the liquid) and to the actual hyperboloidal shape of the liquid bridge surface. They concluded that further experiments should be done to assess the validity of the model, but also noted that, although the predicted resonance frequency was reasonably close to the experimental value, the predicted amplitude of surface oscillations at the resonance frequency was not close to the experimental value.

3. EXPERIMENTAL APPARATUS AND INSTRUMENTATION

A schematic of the new test section is shown in Fig. 1. It had upper and lower disks of 7.0 mm diameter made of brass. In order to reduce the rate of surface evaporation and thinning of the liquid bridge with time, a quartz tube was placed with a gap of 2 ~ 3 mm around the liquid bridge and tightly sealed by placing natural rubber gaskets between the top and bottom ends of the quartz tube and brass bases. Furthermore, a micro-thermocouple used to detect the liquid temperature fluctuations at the onset of oscillatory convection was inserted through a hole in the upper disk to avoid breaking the seal. Thus, the rubber gasket was used to investigate the reduced evaporation case, while it was removed at the top to partially open the system and obtain a relatively high evaporation rate. In both cases, quartz tubes of different lengths were used to change the liquid bridge height and the aspect ratio.

2.1 Disk and Fluid Temperature Measurements

Thermocouples were used to accurately measure the individual disk temperatures, T_H and T_C, the disk temperature difference, ΔT, and liquid temperature, T_f. The liquid temperature fluctuations were measured using a teflon-insulated type-E micro-thermocouple with a wire size of 75 μm inserted into the liquid bridge from the top through a small hole in the upper disk. The details of thermocouple calibration and connection to the data acquisition system can be found in our previous report (Kawaji et al., 2000a).

To sample and record the temperature data nearly free of noise, a PC-based National Instruments Data Acquisition System (Model PCI-6035E with SCXI-1102) was used. For the liquid temperature and ΔT measurements, high-gain, low-noise DC amplifiers (NEC Model 6L06H) were used to amplify the T/C signals before the data acquisition system to maximize the signal-to-noise ratio. All the temperature data were sampled using Labview software at a rate of 10 Hz, stored in files and graphically displayed in real-time.

2.2 Flow Visualization using PIV and Photochromic Dye Activation Techniques

The PIV and photochromic dye activation techniques were used to measure the bulk flow pattern and surface velocity in acetone liquid bridges, respectively. For PIV, a vertical laser light sheet illuminated the silver-coated tracer particles of 8 ~ 12 μm diameter and specific gravity of 1.05 ~ 1.15. The surface velocities on acetone bridges were measured using a photochromic dye activation technique. The details of both flow visualization methods can be found elsewehere (Kawaji et al., 2000a; Kawaji et al., 2000b).

Experiments for 7 mm diameter liquid bridges were performed with the new test section with either a tightly sealed or partially open quartz tube enclosure placed around the liquid bridge. Even for the tightly sealed case, the liquid bridge volume was found to decrease with time due to evaporation, although the rate of volume reduction was about 4 to 5 times less than in the partially open case. Thus, in the remainder of this paper, the experiments will be referred to as reduced evaporation (or closed) case and strongly evaporating (or partially open) case. In each case, the main parameter varied in the experiments was the aspect ratio, $\Gamma = H / R$. In each run, the liquid was injected into the bridge to maximize the initial volume ratio and then the disk temperature difference, ΔT, was either increased or decreased slowly by changing the voltage supplied to the Peltier element attached to the lower (cold) disk, while the upper (hot) disk temperature was kept nearly constant at 23 ~ 25 ^oC. The disk temperature difference, ΔT, was varied as slowly as possible at a relatively constant rate to cross the critical temperature difference and achieve transition from steady to oscillatory flow or vice versa before the volume ratio decreased to less than about 80 - 90% due to evaporation.

Although the liquid bridge was surrounded by a quartz tube and not directly exposed to the ambient atmosphere, fresh liquid was injected to overflow from the lower disk and renew the liquid bridge surface at the beginning of each measurement in order to avoid obtaining data with a contaminated bridge surface.

2.3 Surface Temperature Measurement

To observe the surface temperature distribution, an infrared imager (Inframetrics Model 760) was used together with a rectangular glass enclosure with a zinc-selenide window instead of a quartz tube to surround the liquid bridge. The infrared transmitting characteristics of zinc-selenide (65% ~ 70% transmission at wavelengths between 0.8 μm and 14 μm) allowed measurements of the surface temperature distribution and its variations.

2.4 Horizontal Vibration Tests

A PC-controlled vibration stage (Parker-Daedal Model 404XR150MP) was employed to impose horizontal vibrations to an acetone bridge and find the response of the free surface. The acetone test section was mounted on the stage, which was translated horizontally at a frequency between 1 and 15 Hz, and an acceleration level of 5 mG (5/1000th of normal gravity). A video camera and a 1-axis accelerometer were mounted on the same stage to monitor the acetone bridge motion and acceleration level, respectively. A laser displacement meter (Keyence Model LB1010) with a minimum resolution of 2 μm was also used to measure the position of the test section in a fixed frame of reference.

During the experiment, the liquid evaporated from the acetone bridge so that the ratio of the minimum liquid bridge diameter to the disk diameter (D_{min}/D) decreased continuously with time. This allowed measurements of the free surface response at different volume ratios. The vibration tests were conducted by increasing the applied vibration frequency in steps of 1 Hz and adjusting the translation amplitude to provide an acceleration level of 5 mG.

3. RESULTS AND DISCUSSION

3.1 Evaporation rates for acetone and methanol

The shape of the liquid bridge and the instantaneous volume ratio were obtained from the video images using an image analysis program on a PC. The interface shape was first digitized and the local radius of the liquid bridge was calculated from the free surface coordinates at different heights above the lower disk. The instantaneous liquid bridge volume, V, was then calculated by numerically integrating the local radius-height data, and the volume ratio was obtained as $V = V / \pi R^2 H$. By measuring the volume ratios at the beginning ($V > 100\%$) and after a sufficient amount of time has elapsed, the average evaporation rate could be quantified as % volume reduction per unit time. The evaporation rate data for different aspect ratios are shown for both the closed and partially open systems in Fig. 2. In both systems, the evaporation rate decreased with the increasing aspect ratio, Γ. At all aspect ratios, the partially open system had about 4 ~ 5 times higher evaporation rates than those for the closed system. Also shown in Fig. 2 is the fully open system for $\Gamma = 1.1$, which indicates that fully exposing the acetone bridge to the ambient air increases the evaporation rate by about 7 times when compared to the closed system.

As is clear from the above, even the tightly sealed case showed the effect of surface evaporation and gradual thinning of the acetone bridge with time, although the rate of evaporation was significantly reduced compared to the partially and fully open cases. Mass transfer from the bridge surface continued to occur even in the closed system because the system was not isothermal and temperature differences existed between the liquid surface and the rest of the solid surfaces.

On the other hand, the evaporation rates for a methanol bridge with D = 7.0 mm and an aspect ratio of 1.1 showed only a small difference: 0.05%/sec for the closed system and 0.07%/sec for the partially open system. This means that regardless of the tightness of the seal, the liquid evaporated at similar rates from the methanol bridge surface.

3.2 Effects of evaporation on the surface temperature distribution

The temperature distributions on the acetone bridge surface measured by an infrared imager under steady flow conditions showed significant differences between the closed and

partially open systems, as a result of different rates of evaporative cooling. At reduced evaporation rates in a closed system, the surface temperature distribution was rather uniform as shown in Fig. 3a. As the evaporation rate increased by a factor of 4 to 5 in the partially open system, the surface was cooled to such an extent that a part of the surface became even cooler than the lower cold disk. This can be observed in Fig. 3b as a cold band just above the lower disk, and in a temperature profile along the centerline as shown in Fig. 3c. The latter figure shows the surface temperature relative to the coldest spot on the surface. The error bars indicate the width of the color scale of the infrared imager and the region of uniform temperature indicated by a given color band in the infrared image. The maximum difference between the highest and lowest surface temperatures detected was significantly larger than the disk temperature difference.

The evaporative cooling effect intensified further when a quartz tube was removed from the test section and the acetone bridge was fully exposed to the ambient air as shown in Figs. 4a and 4b. Thus, in both the partially and fully open systems, the cold disk temperature was higher than that of the coldest part of the liquid bridge, indicating an inversion in the temperature gradient near the cold disk, as predicted previously by a linear stability analysis (Nienhuser et al., 2000).

3.3 Determination of critical temperature differences

At the onset of oscillatory Marangoni convection, the fluid temperature measured by a micro-thermocouple started to show harmonic fluctuations with amplitudes of 0.01 ~ 0.1 K and frequencies of about 0.5 ~ 1.0 Hz, as determined from power spectrum analyses. The temperature fluctuation plots were prepared by first taking moving averages of the instantaneous temperature data and subtracting this mean value from the instantaneous temperature to obtain the fluctuating component as a function of time. Sample data for D = 7.0 mm and Γ = 1.1, are shown in Figs. 5 and 6 for the closed and partially open systems, respectively. Both data indicate a gradual increase in the liquid temperature oscillation amplitude well beyond the noise level at the onset of oscillatory flow.

3.4 Surface velocity fluctuations

As a pulse of the UV laser beam was shot on the liquid surface just below the upper disk, a purple-colored dye trace formed instantaneously and moved downward. Although the UV beam penetrated into the liquid and created a short line trace normal to the free surface, the trace appeared initially as a single spot when viewed from outside, parallel to the beam direction. As the surface liquid moved downward due to a shear stress caused by the surface-tension gradient, so did the dye trace. The bottom tip of the trace observed can be considered to represent the surface velocity because fluid elements on the surface are exposed to the maximum intensity of UV light and the trace always reached close to the lower disk.

For the closed system, the dye traces formed near the upper disk in steady flow at $\Delta T < \Delta T_c$, always traveled vertically down to the same azimuthal position near the lower disk indicating an axisymmetric flow. But at the onset of oscillatory flow, the dye trace trajectory started to fluctuate in the azimuthal direction, towards both the left and right of the vertical trajectory as illustrated in Fig. 7. This surface velocity fluctuation from a purely one-dimensional (downward) trajectory to a two-dimensional trajectory with an azimuthal component was observed to occur nearly simultaneously with the appearance of liquid temperature fluctuations described previously. The azimuthal component of the surface velocity changed its direction and magnitude continuously. The ratio of the azimuthal component to the vertical component of surface velocity was found to be about 30 degrees at

ΔT = 0.85 K, well above the critical ΔT of 0.5 K.

3.5 Vortex expansion and contraction

In PIV images of the flow patterns in the vertical cross section, a pair of vortices appeared near the liquid bridge surface as shown in Fig. 8, representing a toroidal vortex. At the onset of oscillatory flow, these vortices started to expand and contract as shown in Fig. 8a – 8c at the same frequency as the temperature oscillations, as previously reported by Chun and Wuest (1979), among others.

3.6 Surface temperature variation

For the closed system with a reduced evaporation rate, the surface temperature recorded by an infrared imager showed the propagation of hydothermal waves in the azimuthal direction, shortly after the onset of oscillatory flow. A slightly colder patch moved from right to left (in the clockwise direction) at the same frequency as the liquid temperature oscillations detected by a micro-thermocouple. In the partially open system with enhanced evaporation rates, a cold region appeared above the lower cold disk as mentioned earlier. At the onset of oscillatory flow, this cold region started to fluctuate in position and height with the same frequency as the liquid temperature. Propagation of hydrothermal waves could be seen in the partially open system as well.

3.7 Critical temperature differences and Marangoni numbers at the onset of oscillatory convection

Liquid temperature oscillations detected by one or two micro-thermocouples inserted into the liquid bridge were examined to determine the critical temperature difference, ΔT_c, at the onset of oscillatory flow for various aspect ratios and volume ratios. The liquid temperature fluctuations were plotted against time together with the temperature difference between the hot and cold disks, as shown earlier in Figs. 5 and 6 for the closed and partially open systems, respectively. In both cases, before the onset of oscillatory flow, the liquid temperature data showed random fluctuations of small and constant amplitude of about ± 0.005K, considered to be the background noise. At the onset of oscillatory flow, the liquid temperature oscillations started to grow larger in amplitude showing highly regular periodicity with a certain frequency.

When the disk temperature difference was reduced from above ΔT_c, the periodic temperature oscillations gradually decreased in amplitude and disappeared at a certain ΔT slightly below ΔT_c. This was common to both closed and partially open systems, and is attributed to a finite amount of time necessary for the oscillatory motion to fully decay.

The present analyses of ΔT_c data for D = 7.0 mm and different aspect ratios showed ΔT_c to range from 0.5 K to 1.1 K in the closed system and 1.8 K to 2.6 K for the partially open system (Fig. 9). The data are shown for both increasing ΔT (corresponding to steady to oscillatory transition) and decreasing ΔT (oscillatory to steady transition). The critical ΔT values for increasing ΔT were always greater than those for decreasing ΔT, as previously reported by Velten et al. (1991). Significant differences in the critical ΔT values between the closed and partially open systems even for the same disk diameter and aspect ratio are clearly the result of surface evaporation. The partially open system with a higher rate of surface evaporation became more stable and the onset of oscillatory convection was delayed until much higher values of ΔT_c were reached compared to the closed system.

In all cases, a strong dependence of ΔT_c on the aspect ratio was found. For the closed

system with a disk diameter of 7.0 mm, the value of ΔT_c decreased by more than 50 % as the aspect ratio increased from 0.56 to 1. It then increased slightly for $\Gamma > 1$ so that the minimum ΔT_c of about 0.5 K was reached at $\Gamma \approx 1$. The dependence of ΔT_c on the aspect ratio was rather similar for the partially open system.

The critical Marangoni number, Ma_c, was next calculated based on ΔT_c and the liquid bridge height, H. Velten et al. (1991) used a different definition of the Marangoni number, $Ma_c^* = Ma_c / \Gamma^2$, while many other authors have used Ma_c. The critical Marangoni number data for a volume ratio of about 100% are plotted against the aspect ratio in Fig. 10 for D = 7 mm and both closed and partially open systems. For the closed system with reduced evaporation rates, the critical Marangoni number, Ma_c^*, decreased strongly with the aspect ratio, while Ma_c was nearly constant for $\Gamma < 1$ and increased slightly for $\Gamma > 1$. This indicates that the use of Ma_c is the better choice. Also shown in Fig. 10 are the critical Marangoni numbers for Pr = 4.3 interpolated from Velten et al.'s (1991) data for Pr = 1 and 6.9 obtained for a disk diameter of 6 mm. The critical Marangoni numbers, Ma_c^*, for the closed system and D = 7 mm were found to be consistent with the values interpolated from Velten et al.'s (1991) data.

The critical Marangoni numbers, Ma_c^*, for methanol (Pr = 7, D = 7.0 mm, Γ = 1.1) are shown in Fig. 11 for both the closed and partially open systems. There is little difference between the two systems because of the small difference in the liquid evaporation rates as mentioned earlier. The critical Marangoni number data also agreed well with Velten et al.'s (1992) data for the same Prandtl number.

3.8 Effects of horizontal vibration on liquid bridge motion

The amplitudes of free surface oscillation recorded for an aspect ratio Γ = 1.04 at different vibration frequencies but a constant diameter ratio of $D_{min}/D = 0.76$ are shown in Fig. 12 for the same acceleration level of 5 mG. Several peaks in the maximum amplitude are seen in this figure, indicating the acetone bridge responds to certain applied vibration frequencies (4 and 12 Hz) with larger amplitudes than at other frequencies. These particular vibration frequencies at which the peak surface oscillation amplitudes occur can be considered to be related to the resonance frequencies.

The maximum surface oscillation amplitudes obtained at different diameter ratios are shown in Fig. 13. This figure shows that at any vibration frequency, the free surface oscillated with amplitudes greater than 50 microns. The diameter ratio at which the maximum amplitude occurred ranged from 0.58 to 0.88 as listed in Table 1 and shown in Fig. 14 for various applied vibration frequencies.

At a given applied vibration frequency, the surface oscillation amplitude varied strongly with the liquid bridge volume or diameter ratio. For example, the data shown in Fig. 15 for 4 Hz vibration indicate the maximum amplitude to occur at $D_{min}/D = 0.76$.

The frequencies at which the liquid bridge surface oscillates changed with the applied vibration frequency and diameter ratio as shown in Fig. 16. In the low frequency range, 1 - 6 Hz, the surface oscillated at harmonic frequencies (i.e., 2x, 3x, etc.) and the higher harmonics were observed at larger diameter ratios. Because of the resonance frequency at 12 Hz, in many instances, the surface oscillated at that frequency or close to it regardless of the applied vibration frequency. On the other hand, at high applied vibration frequencies in the range 7 – 15 Hz, the surface oscillated at a frequency equal to the applied vibration frequency, as shown in Table 1.

Finally, the effect of the liquid bridge height on the resonance frequencies was investigated by setting the height at 2.42 mm, 3.67 mm and 4.55 mm (corresponding to aspect ratios of 0.70, 1.04 and 1.30). The observed frequencies at which the maximum surface oscillation amplitude occurs decreased linearly with the liquid bridge height as shown in Fig.

17. Thus, the resonance frequencies are clearly seen to depend on the size (height and most likely the diameter) of the liquid bridge.

3.9 Comparison of acetone vibration results with model predictions

In this section the vibration results are compared with the predictions of the model proposed by Ichikawa et al. (2001) with a value of the parameter B set to 1 as described earlier in Section 2. Table 2 summarizes the resonance frequencies obtained for acetone liquid bridges experimentally and the predictions of the model, which is applicable to perfectly cylindrical liquid bridges. The resonance frequency for the acetone bridge of height H = 3.7mm predicted by the model is 11.2 Hz. In the experiments, resonance was observed to occur at an applied frequency = 12 Hz at a diameter ratio (D_{min}/D) equal to 0.76. For a cylindrical bridge, D_{min}/D = 1, the oscillation amplitude was small, and no significant resonance was found at any frequency. Thus, the model can predict the resonance frequency well, but not the diameter ratio at which resonance occurs.

According to equation 13, the resonance frequency of a liquid bridge is expected to be inversely proportional to the height of the liquid bridge. This prediction was in good agreement with the experimental results.

4. CONCLUSIONS

In acetone liquid bridges with D = 7 mm and 1.5 mm < H < 4.5 mm, the effect of liquid evaporation from the free surface on the transition from steady to oscillatory Marangoni convection was investigated experimentally. The evaporation rate was changed by partially or completely enclosing the liquid bridge with a quartz tube. Using a variety of instrumentation, the following phenomena have been observed to occur at the onset of oscillatory convection regardless of the surface evaporation rate:

- liquid temperature starts to oscillate periodically with amplitudes as small as 0.01K,
- surface velocity starts to fluctuate in the azimuthal direction,
- toroidal vortex below the free surface starts to expand and contract periodically,
- surface temperature pattern shows azimuthally travelling hydrothermal waves.

The surface evaporation was observed to significantly cool the acetone bridge and alter the surface temperature distribution in both steady and oscillatory flows. For the partially open and fully open systems, a cold surface region appeared above the lower cold disk, with a temperature below that of the cold disk, indicating a temperature inversion as predicted by a linear stability analysis.

The critical temperature difference, at which the flow becomes oscillatory, was found to depend strongly on the evaporation rate. The critical temperature difference also varied strongly with the aspect ratio (height / radius) ranging from 0.5 to 1.05 K for the closed system with D = 7 mm, while it ranged from 1.6 to 2.3K for the partially open system (strongly evaporating case). The present critical Marangoni number data for acetone bridges with D = 7 mm in a closed system were consistent with the values for Pr = 4.4 interpolated from Velten et al.'s (1991) data for Pr = 1 and 7 and D = 6 mm. Because of low evaporation rates, the critical Marangoni number data for methanol (Pr = 7, D = 7.0 mm) for an aspect ratio close to 1 in both closed and partially open systems were also similar to the values reported by Velten et al. (1991) for $NaNO_3$ (Pr = 7). Thus, the effect of liquid evaporation on Marangoni convection was to stabilize the flow and increase the critical temperature difference required for transition from steady to oscillatory convection.

The horizontal vibrations applied to an acetone bridge with a 7.0 mm disk diameter were found to cause significant oscillations of the free surface, especially when the applied vibration frequency is related to the resonance frequencies (e.g., 4 and 12 Hz for an aspect ratio of 1.04). The maximum amplitude of the free surface oscillation was found to occur at different volume ratios and reach more than 250 μm at the resonance frequencies. The resonance frequencies were found to decrease linearly with the aspect ratio.

REFERENCES

Chun, Ch.-H. and Wuest, W., 1979, "Experiments onthe transition from the steady to the oscillatory Marangoni-convection of a floating zone under reduced gravity effect," Acta Astronautica, Vol. 6, pp.1073-1082.

Ichikawa, N., Misawa, M. and Kawaji, M., 2001. Resonance behavior of liquid bridge caused by small vibration. Proc. of 4th International Conference on Multiphase Flow, New Orleans, Louisiana, USA. May 27 - June 1, 2001.

Kamotani Y., Ostrach, S. and Vargas, M., 1984, "Oscillatory thermocapillary convection in a simulated float-zone configuration", J. Crystal Growth, Vol. 66, pp. 83- 90.

Kawaji, M., Otsubo, F., Simic, S. and Yoda, S., 2000a, "Transition to oscillatory Marangoni convection in liquid bridges of intermediate Prandtl number," Annual Report on Marangoni Convection Modeling Research, NASDA Technical Memorandum, September, 2000, National Space Development Agency of Japan, pp.75-114.

Kawaji, M., Otsubo, F. And Yoda, S., 2000b, "Transition to Oscillatory Marangoni Flow in Liquid Bridges of Intermediate Prandtl Number," Paper NHTC2000-12200, Proc. of the 34th National Heat Transfer Conference, Pittsburgh, Pennsylvania, August 20-22, 2000.

Leypoldt, J., Kuhlmann, H.C.and Rath H.J., 2000. Three-dimensional numerical simulation of thermocapillary flows in cylindrical liquid bridges, Journal of Fluid Mechanics, v. 414, pp. 285-314.

Nienhuser, Ch., Kuhlmann, H.C., Rath, H.J., and Yoda, S., 2000, "Linear stability of the two-dimensional flow in half-zones: The influence of free surfcae heat transfer, aspect ratio and volume of liquid," Annual Report on Marangoni Convection Modeling Research, NASDA Technical Memorandum, September, 2000, National Space Development Agency of Japan, pp. 215-246.

Preisser, F., Schwabe, D. And Scharmann, A., 1983, "Steady and oscillatory thermocapillary convection in liquid columns with free cylindrical surface", J. Fluid Mechanics, Vol. 126, pp. 545-567.

Vargas, M., 1982, "Oscillatory thermocapillary flow in a simulated floating-zone configuration," M.Sc. thesis, Case Western Reserve University.

Velten, R., Schwabe, D. and Scharmann, A., 1991, "The periodic instability of thermocapillary convection in cylindrical liquid bridges", Phys. of Fluids, A., Vol. 3 (2), pp. 267-279.

Wanschura, M., Shevtsova, V.M., Kuhlmann, H.C., and Rath, H.J., 1995, "Convective instability mechanisms in thermocapillary liquid bridges," Phys. Fluids, 7(5), pp. 912-925.

Table 1 Variation of surface oscillation frequency and diameter ratio at maximum amplitude with the applied vibration frequency

Frequency of Applied Vibration (Hz)	Diameter Ratio (D_{min}/D)	Surface Oscillation Frequency (Hz)
1	0.88	13
2	0.71	10
3	0.65	9
4	0.76	12
5	0.71	10
6	0.79	12
7	0.58	7
8	0.61	8
9	0.65	9
10	0.69	10
11	0.72	11
12	0.76	12

Table 2 Comparisons of measured and predicted resonance frequencies (acetone, D = 7.0 mm)

Bridge Height H	Measured resonance frequency (Hz) and diameter ratio	Predicted resonance frequency (Hz) (D_{min}/D = 1 assumed)
2.42 mm	16 at D_{min}/D = 0.76	17.0
3.67 mm	12 at D_{min}/D = 0.76	11.2
4.55 mm	10 at D_{min}/D = 0.76	9.1

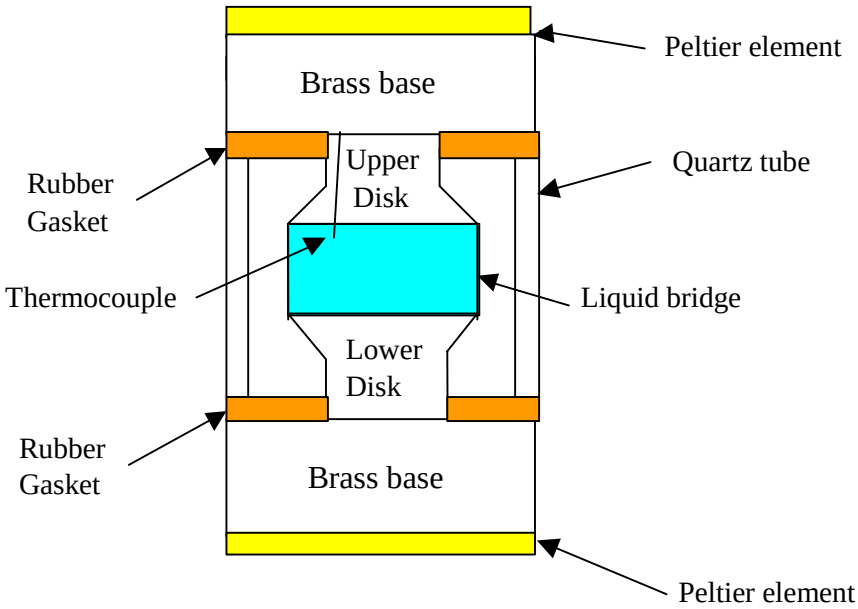

Fig. 1 Schematic of a new test section

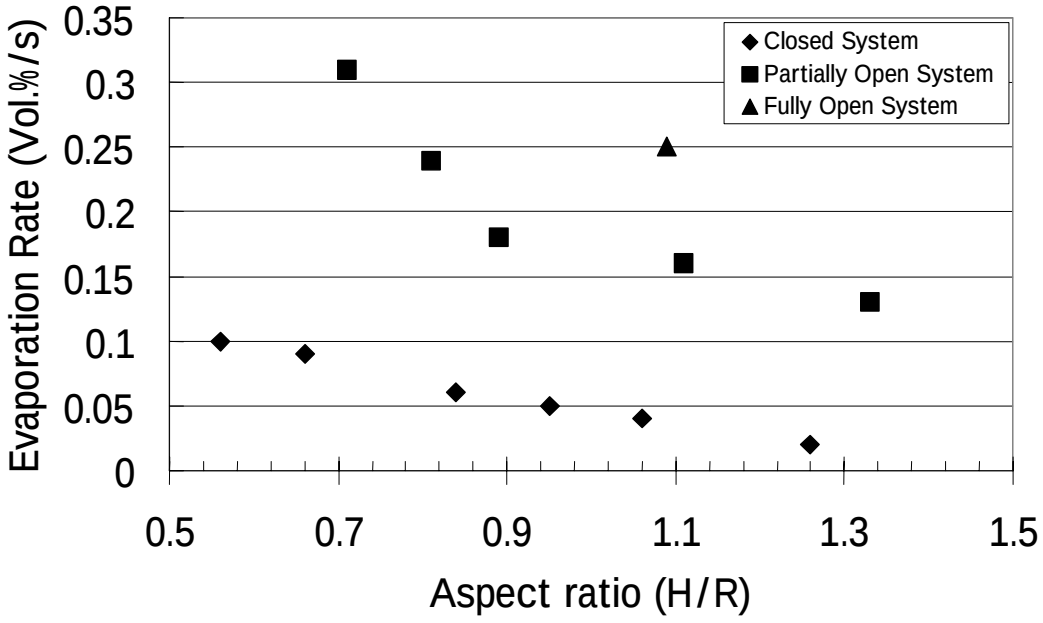

Fig. 2 Variation of evaporation rates with aspect ratio for closed and partially open systems (acetone, D = 7.0 mm)

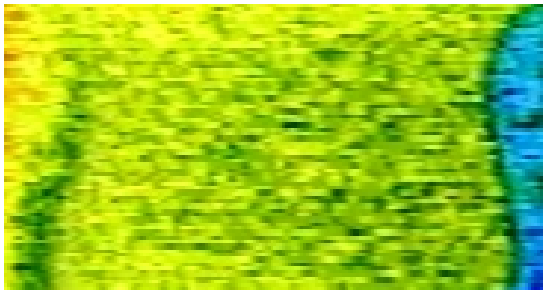

(a)

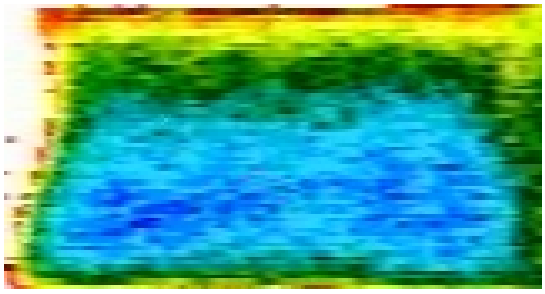

(b)

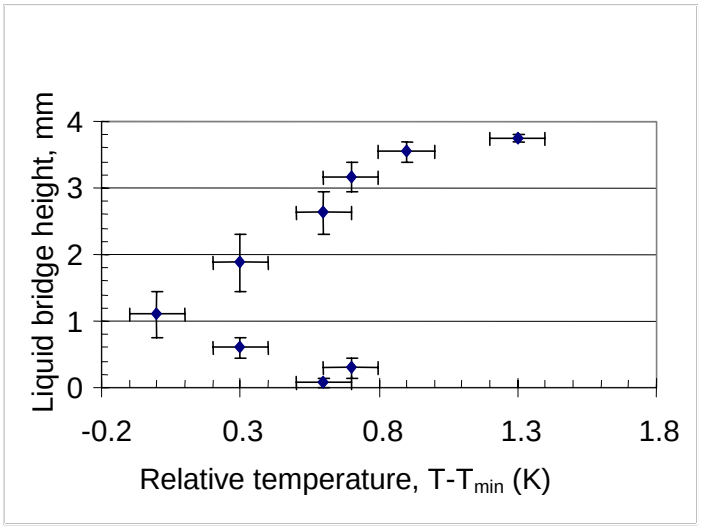

(c)

Fig. 3 Surface temperature distribution for D = 7 mm, Γ = 1.1: (a) IR image for a closed system, (b) IR image for a partially open system, and (c) temperature profile along the centerline.

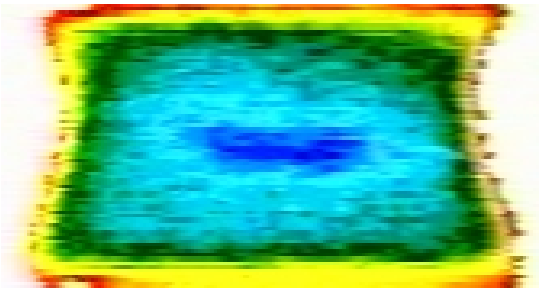

(a)

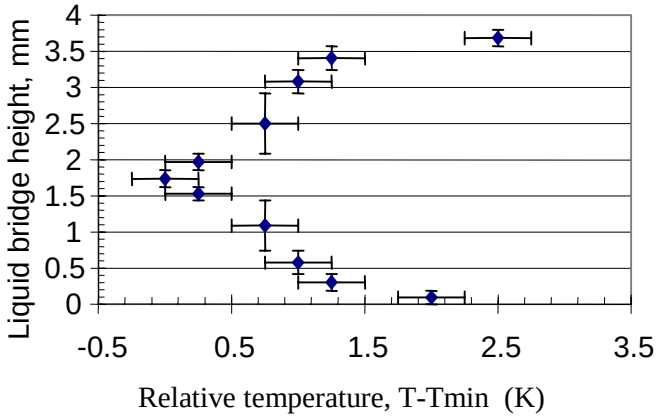

(b)

Fig. 4 Surface temperature distribution for D = 7 mm, Γ = 1.1: (a) IR image for a fully open system at ΔT = 0.6 K, and (b) temperature profile along the centerline.

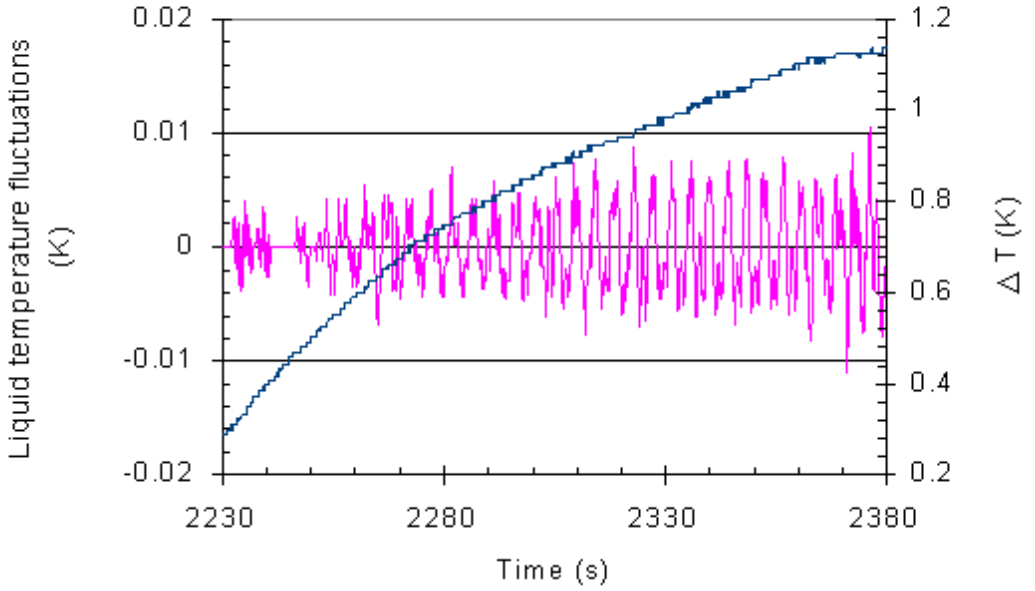

Fig. 5 Liquid temperature oscillations at the onset of oscillatory convection (Closed system, D = 7.0 mm, Γ = 1.1)

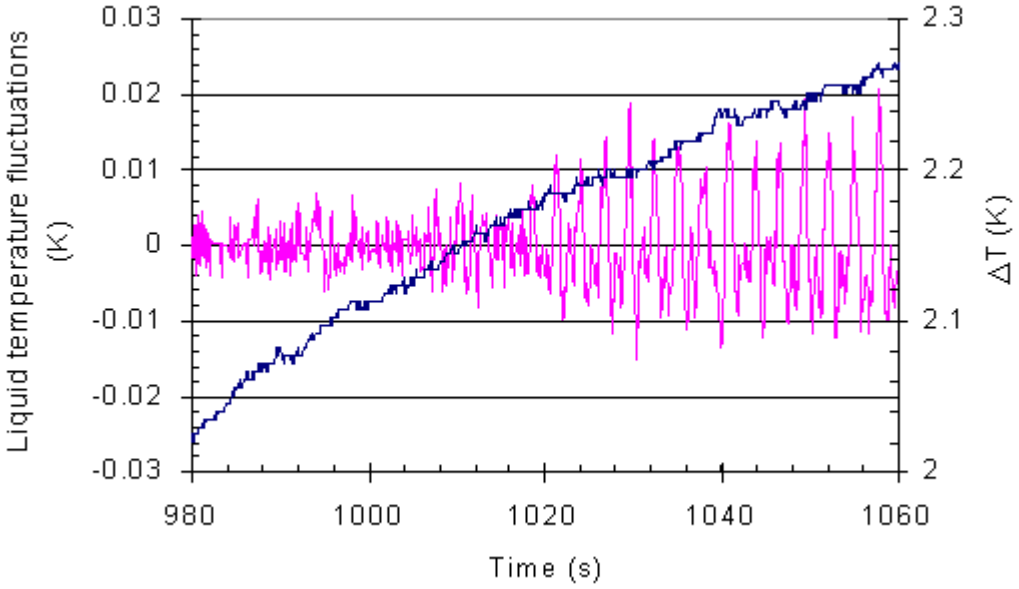

Fig. 6 Liquid temperature oscillations at the onset of oscillatory convection (Partially open system, D = 7.0 mm, Γ =1.1)

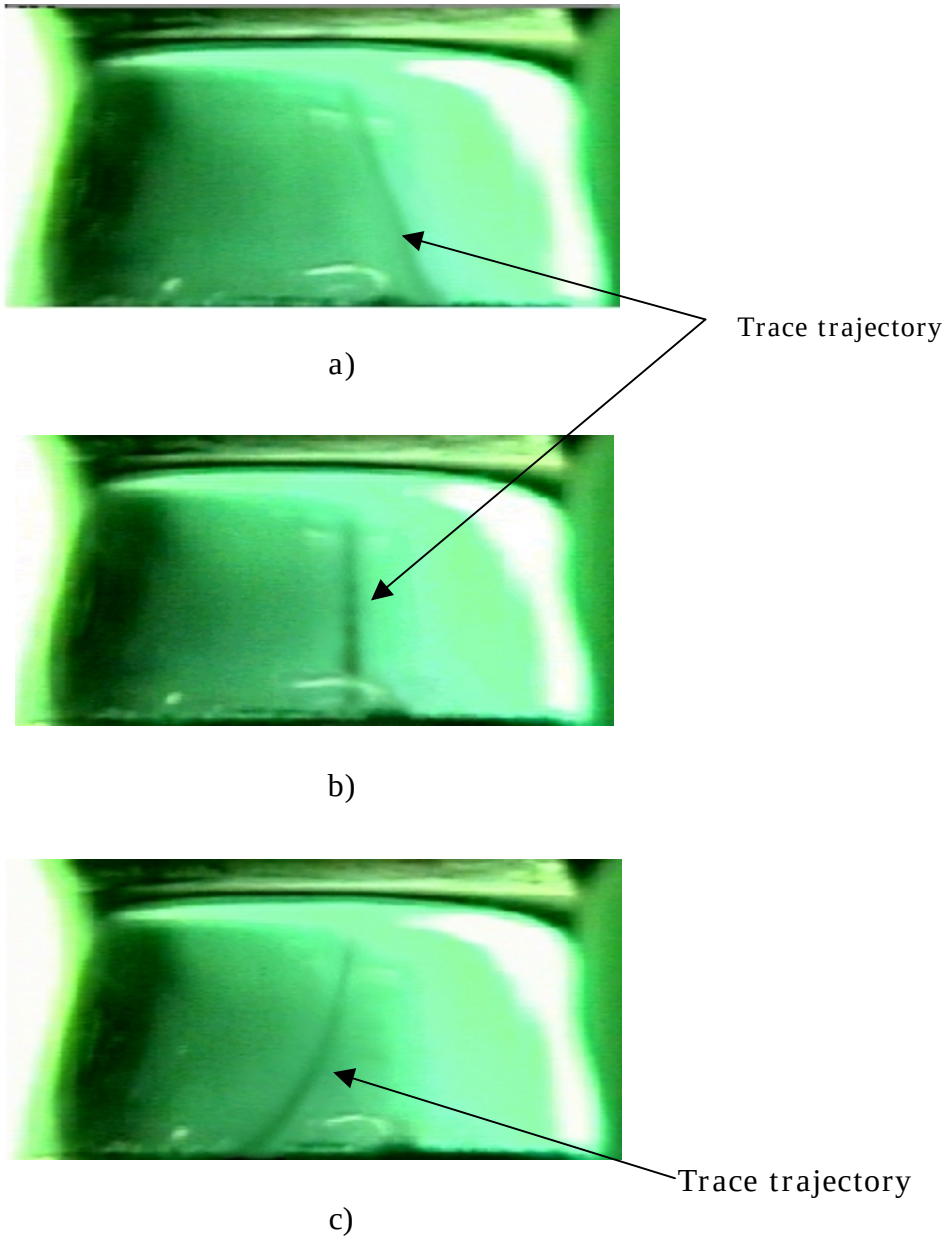

Fig. 7 Phtotochromic dye trace images (enhanced) indicating the surface flow direction during oscillatory Marangoni convection in an acetone liquid bridge
(closed system, D = 7.0 mm, Γ =1.1, ΔT = 0.85 K)

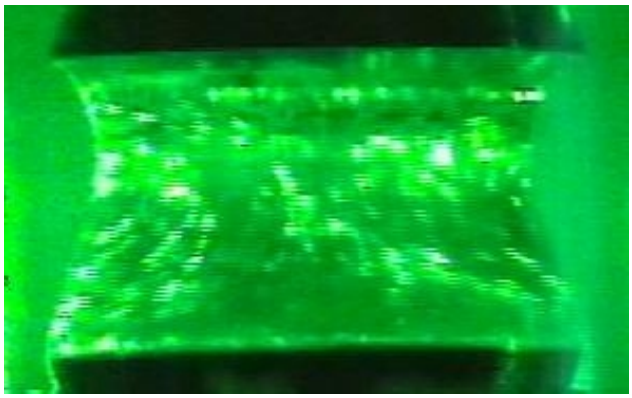

a)

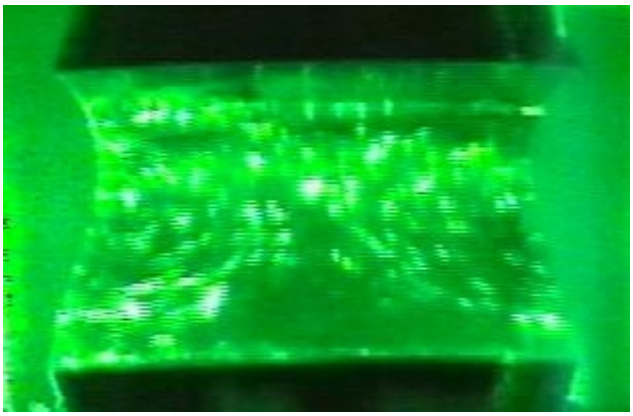

b)

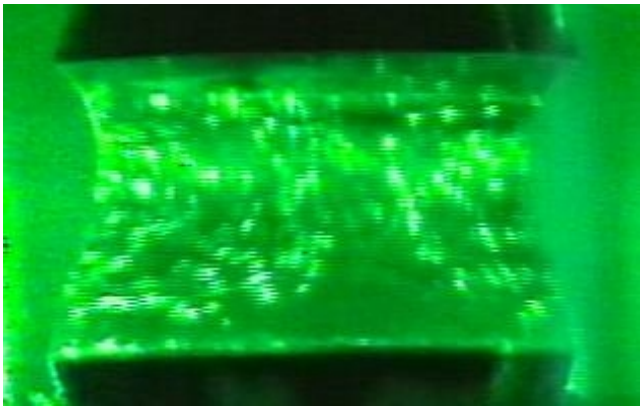

c)

Fig. 8 PIV images of expanding and contracting vortices during oscillatory Marangoni convection in an acetone liquid bridge
(closed system, D = 7.0 mm, Γ =1.1, ΔT = 1.57 K)

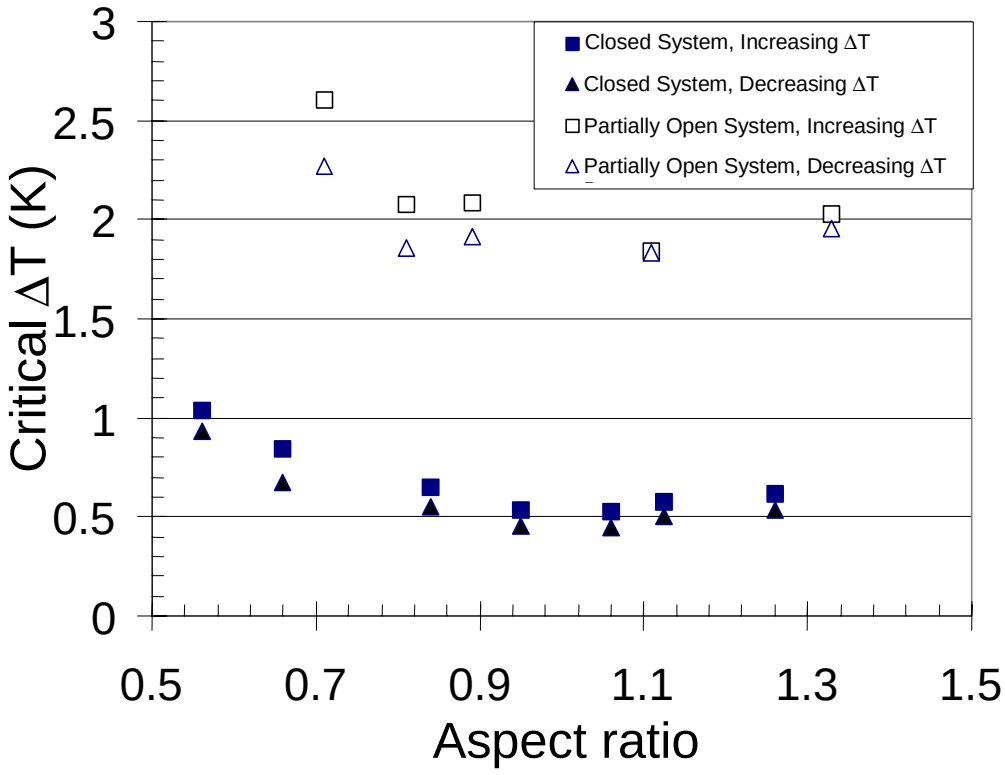

Fig. 9 Critical disk temperature differences at the onset of oscillatory Marangoni convection (acetone bridge, D = 7.0 mm)

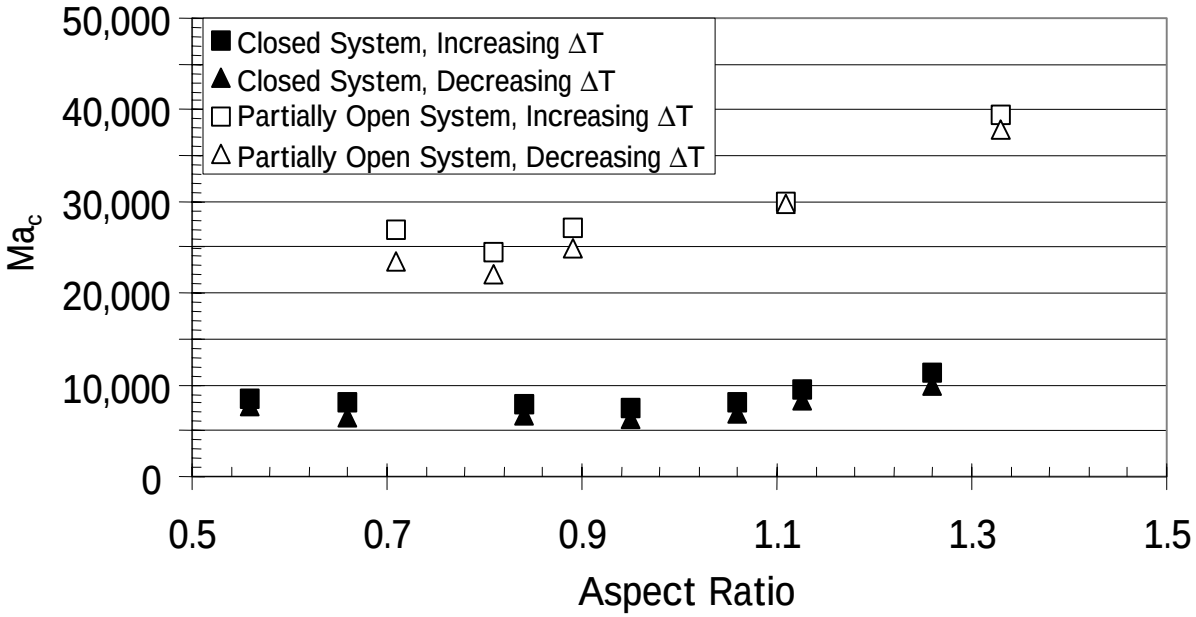

(a)

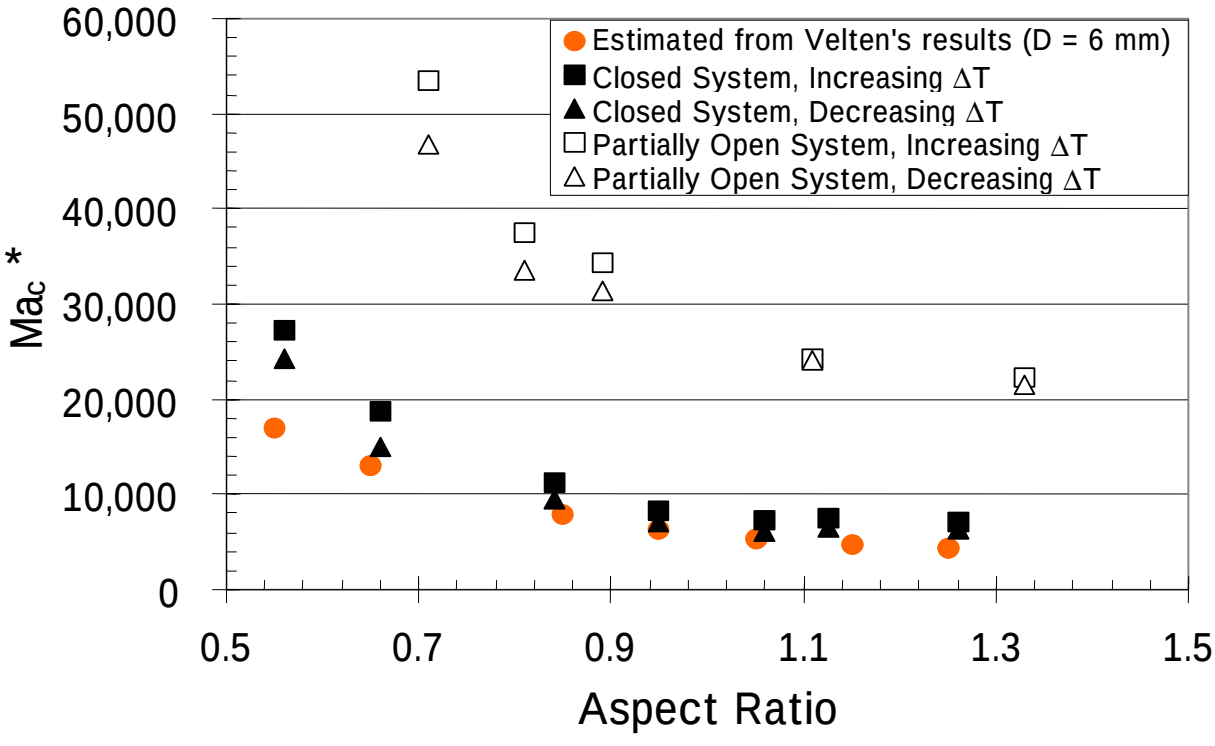

(b)

Fig. 10 Variation of critical Marangoni numbers (a) Ma_c and (b) Ma_c^* with aspect ratio (D = 7 mm in closed and partially open systems)

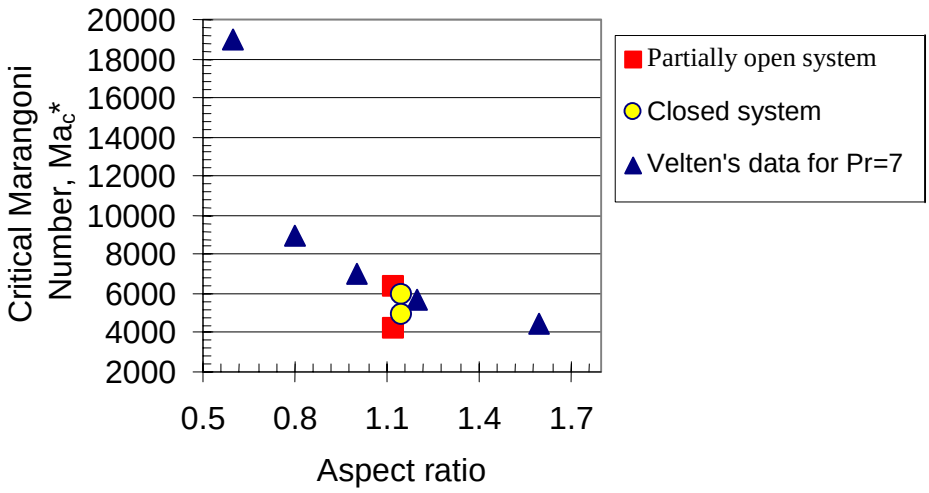

Fig. 11 Comparison of critical Marangoni number, Ma_c*, data for methanol (D = 7.0 mm, Γ = 1.1, Pr = 7) with Velten et al.'s data for D = 6.0 mm and Pr = 7

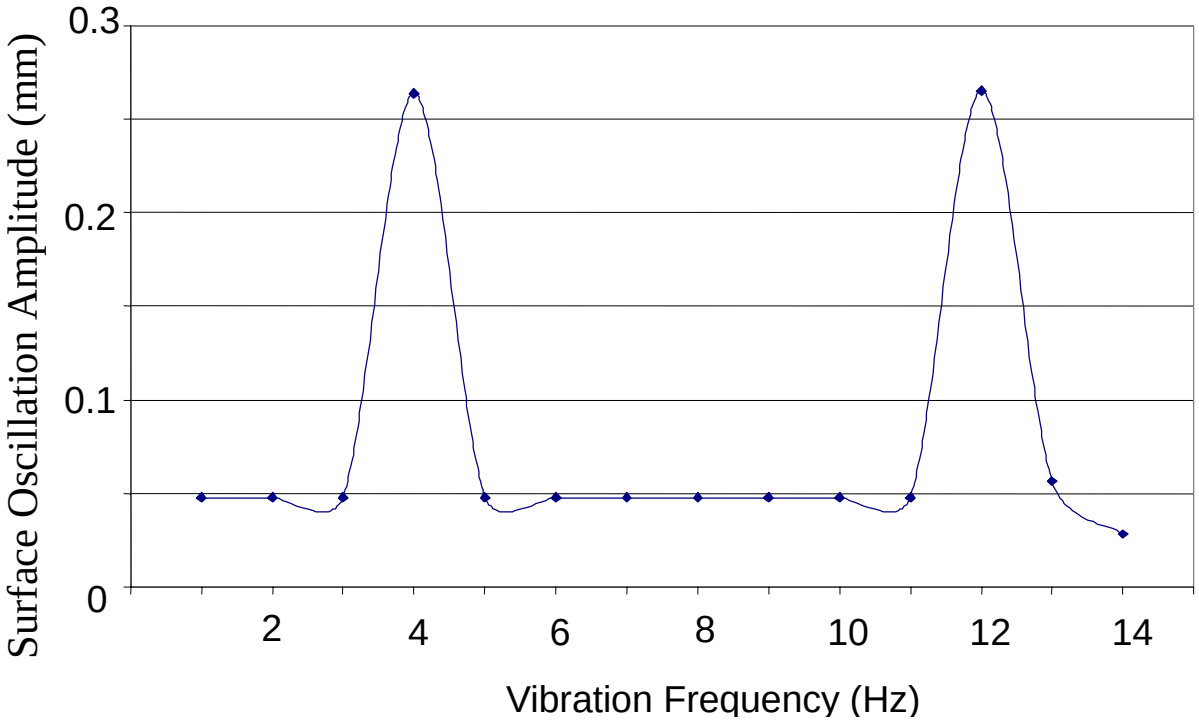

Fig. 12 Surface oscillation amplitudes of acetone bridge (D = 7.0 mm, Γ = 1.04, D_{min}/D = 0.76)

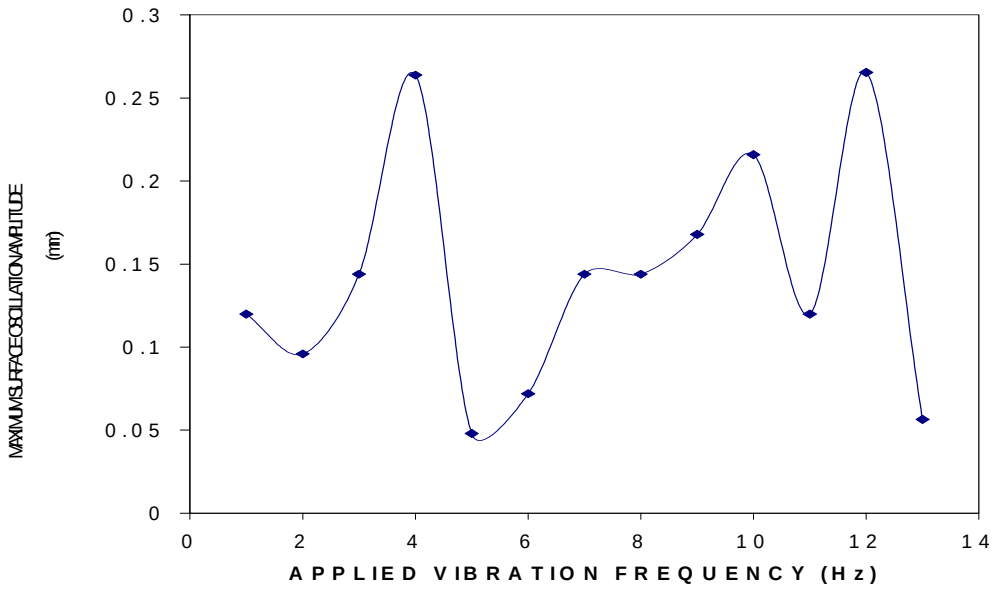

Fig. 13 Variation of maximum surface oscillation amplitudes of acetone bridge with the applied vibration frequency for D = 7.0 mm, Γ = 1.04, and 5 mG acceleration

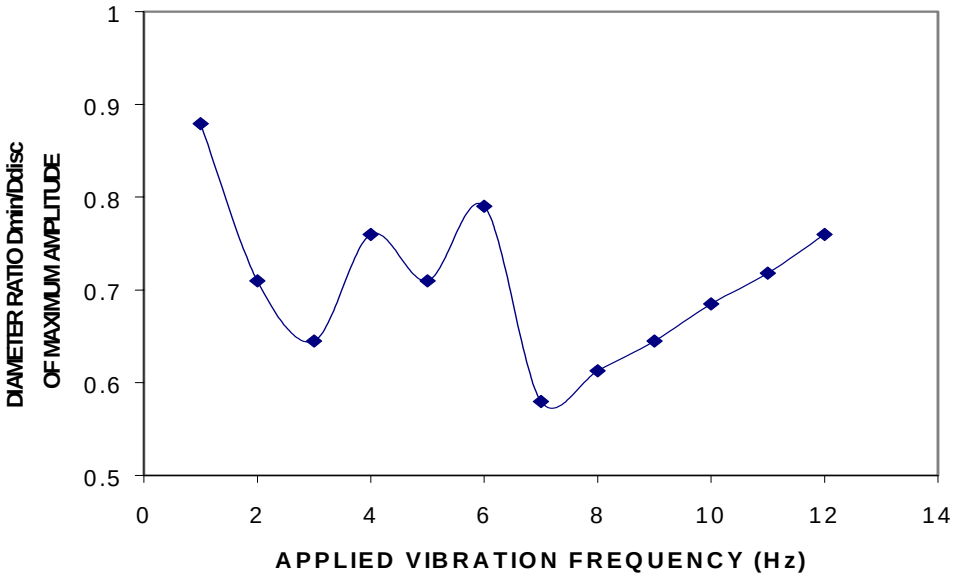

Fig. 14 Diameter ratio at which maximum surface oscillation amplitude occurred at different applied vibration frequencies in an acetone bridge for D = 7.0 mm, Γ = 1.04, and 5 mG acceleration

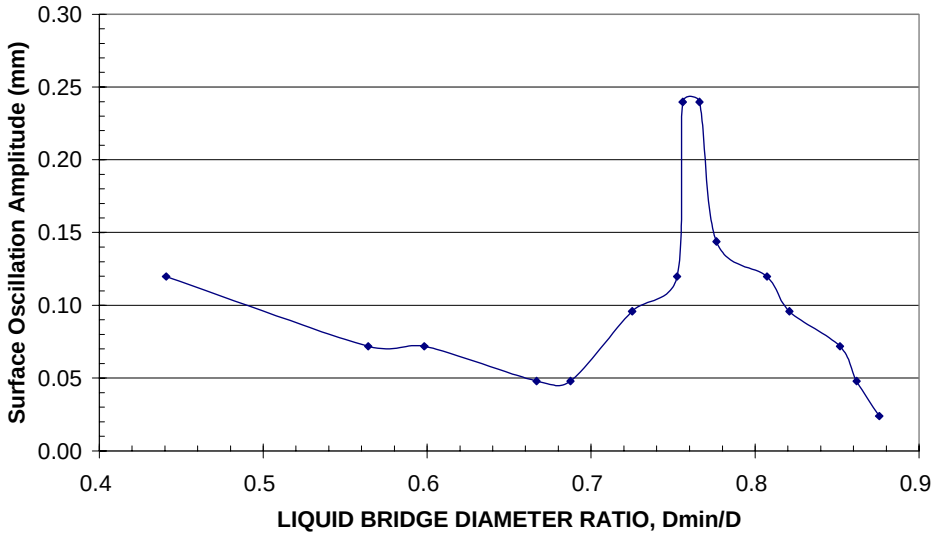

Fig. 15 Variation of surface oscillation amplitudes of acetone bridge with the diameter ratio, D_{min}/D, for D = 7.0 mm, Γ = 1.04, 5 mG acceleration and 4 Hz vibration frequency

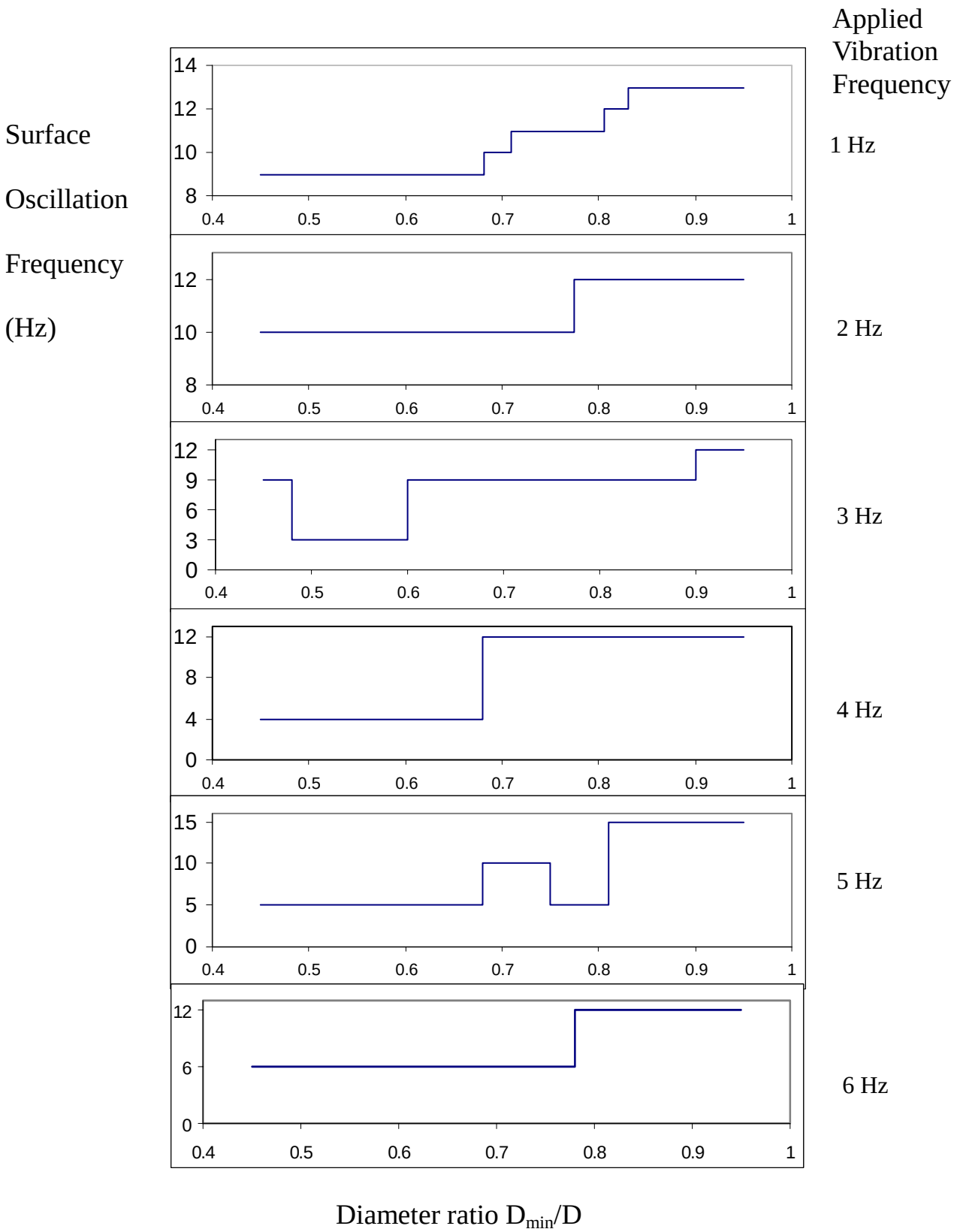

Fig. 16 Variation of observed surface oscillation with the diameter ratio for low applied vibration frequencies (acetone bridge, D = 7.0 mm, 5 mG acceleration)

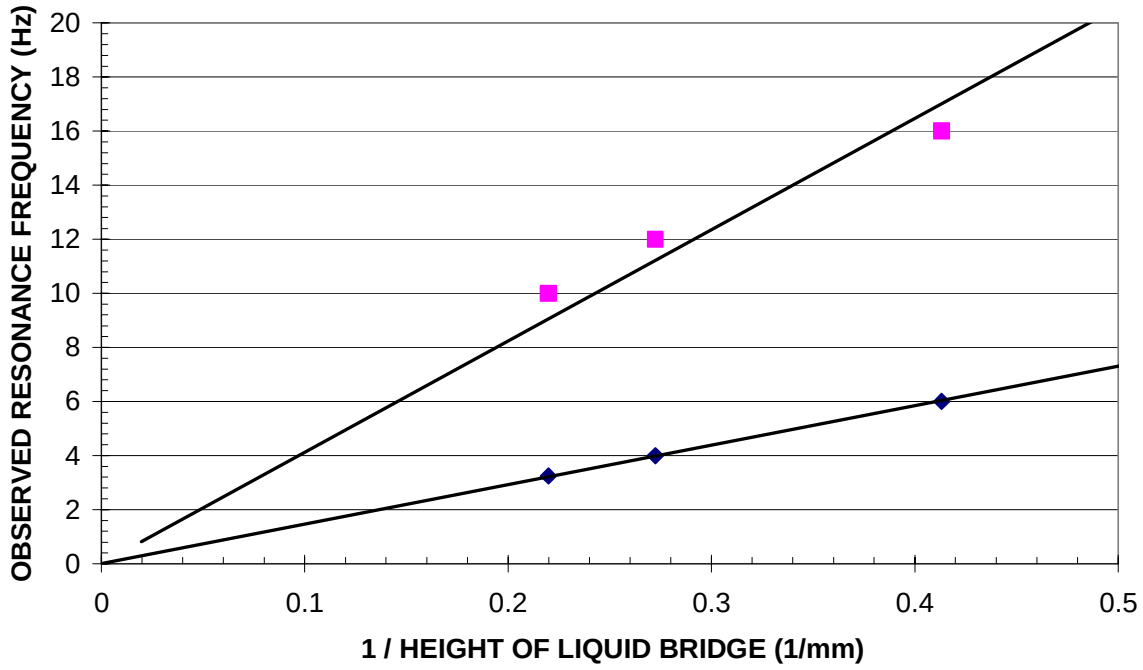

Fig. 17 Variation of the resonance frequencies with the liquid bridge height (acetone, D = 7.0 mm, 5 mG acceleration)